




De novo evolution of antibiotic resistance to Oct-TriA₁

Farhan R. Chowdhury^{a,1}, Laura Domínguez Mercado^{b,1}, Katya Kharitonov^a,
Brandon L. Findlay^{a,b,*} 

^a Department of Biology, Concordia University, Montréal, Québec H4B 1R6, Canada

^b Department of Chemistry and Biochemistry, Concordia University, Montréal, Québec H4B 1R6, Canada

ARTICLE INFO

Keywords:

Antibiotic resistance
Tridecaptin
Soft agar gradient evolution
Synaeresis
Lipopeptides
Xanthan gum
Evolution-resilient antibiotics

ABSTRACT

The rise of antimicrobial resistance as a global health concern has led to a strong interest in compounds able to inhibit the growth of bacteria without detectable levels of resistance evolution. A number of these compounds have been reported in recent years, including the tridecaptins, a small family of lipopeptides typified by the synthetic analogue octyl-tridecaptin A₁. Hypothesizing that prior reports of negligible resistance evolution have been due in part to limitations in the laboratory evolution systems used, we have attempted to select for resistant mutants using a soft agar gradient evolution (SAGE) system developed by our lab. Following optimization of the media conditions by incorporation of the anti-synaeresis agent xanthan gum into the agar matrix, we successfully evolved high-level resistance to both octyl-tridecaptin A₁ as well as the challenging lipopeptide antibiotic polymyxin B. Decreased tridecaptin susceptibility was linked to mutations in outer membrane proteins *ompC*, *lptD* and *mlaA*, with the effect of these genes confirmed through a mix of allelic replacement and knockout studies. Overall, this work demonstrates the robust evolutionary potential of bacteria, even in the face of challenging antimicrobial agents.

1. Introduction

Antimicrobial resistance (AMR) is a major global health concern that threatens access to basic medical interventions. It is estimated that AMR was directly responsible for 1.27 million global deaths and contributed to 4.95 million deaths in 2019 (Murray et al., 2022), and it is currently projected that, if left unchecked, AMR will be responsible for 10 million deaths annually by 2050 (Jacobs, 2019).

Unfortunately, resistance to many potential new antibiotics can be found in bacterial pathogens before the drugs' commercial release, due in part to cross-resistance between similar drug molecules (Bonomo et al., 2024). Studies that describe new antibiotics now often include adaptive laboratory evolution (ALE) experiments to determine rates of resistance or to elucidate the mechanism of action, with some antibiotics showing little to no resistance evolution (Mcguire et al., 1955; Ge et al., 1999; Ling et al., 2015; Cochrane et al., 2016; Stokes et al., 2020; Shukla et al., 2022). These latter antibiotics have attracted significant interest as promising candidates for next-generation antibiotic therapy, and may represent desirable "evolution-proof" or "resistance-proof" agents (Bell and MacLean, 2018; Upadhayay et al., 2023). However, the

evolutionary resilience of many of these compounds has only been assessed through a limited array of ALE experiments, and has generally not been independently verified.

Tridecaptin A₁ is one antibiotic against which laboratory evolution experiments have failed to describe *de novo* resistance. Originally isolated from *Paenibacillus* spp. (Shoji et al., 1978; Lohans et al., 2012), the tridecaptins are a group of non-ribosomal lipopeptides that act by selectively binding to the cell wall synthesis precursor lipid II of Gram-negative bacteria and dissipating the proton motive force (Cochrane et al., 2016). Their linear structure is readily accessible to solid phase peptide synthesis, allowing facile construction of tridecaptin analogues (Cochrane et al., 2014b; Ballantine et al., 2019). Best studied of these is octyl-tridecaptin A₁ (Oct-TriA₁), in which the chiral lipid tail is replaced with a low-cost octyl equivalent with no significant change in antimicrobial activity (Cochrane et al., 2014a). Tridecaptins are selective for Gram-negative bacteria, and their potent activity against the majority of the WHO's priority pathogens list (WHO, 2023) makes them exciting antibiotic candidates. They have also been reported to be evolutionarily resilient, with Cochrane et al. finding no appreciable resistance to Oct-TriA₁ following a 30-day laboratory evolution

* Corresponding author at: Department of Biology, Concordia University, Montréal, Québec H4B 1R6, Canada.

E-mail address: brandon.findlay@concordia.ca (B.L. Findlay).

¹ These authors contributed equally to this work.

experiment (Cochrane et al., 2016).

Gram negative bacteria are notoriously difficult to treat, and some recent efforts have focused on targeting the very outer membrane that makes them more resilient. Some examples of such antibiotics include compounds that inhibit LPS biosynthesis or transport, like cerastecin (Wang et al., 2024), zosurabalpin (Zampaloni et al., 2024) and analogs (Pahil et al., 2024), L27-11 (Werneburg et al., 2012), murepavadin (Srinivas et al., 2010), IMB-881 (Zhang et al., 2019). Likewise, antibiotics like darobactin (Imai et al., 2019) target OM proteins (Kaur et al., 2021). This strategy seems to confer certain selectivity, enabling narrow-spectrum antibiotics and which may reduce the likelihood of developing resistance (Srinivas et al., 2010; Werneburg et al., 2012; Zampaloni et al., 2024; Wang et al., 2024). These antibiotics are especially interesting as their resistance could also lead to loss of virulence, by directly targeting LPS and OM stability (Imai et al., 2019).

We previously reported the ability of the soft agar gradient evolution (SAGE) system to rapidly generate resistance against antibiotics, including ones difficult to evolve in other platforms (Ghaddar et al., 2018). SAGE uses antibiotic gradients and bacteria's natural propensity to swim through soft agar to select for antibiotic-resistant mutants. Unfortunately, the efficacy of SAGE is limited by syneresis, the tendency of agar hydrogels to spontaneously shrink over time via continuous expulsion of solvent (Divoux et al., 2015). In SAGE this hinders bacterial motility (Croze et al., 2011) and limits experiments to ten days or less. We report here a new SAGE medium that is resistant to syneresis. Supplemented with xanthan gum, a polysaccharide with excellent water binding capacity (Sánchez et al., 1995), this media has a reduced

agar content and is suitable for month-long evolution experiments. We start by showing that resistance to the lipopeptide polymyxin B (PolB), an antibiotic that has proven difficult to evolve resistance to in SAGE (Ghaddar et al., 2018) and in other platforms (Trimble et al., 2016), can now be quickly achieved via SAGE. We subsequently use this medium to successfully generate resistance against Oct-TriA₁ in *Escherichia coli* through a 27-day, maintenance free, SAGE experiment. Whole genome sequencing of evolved strains reveals mutations in phospholipid transport, outer membrane (OM) assembly and lipopolysaccharide (LPS) biosynthesis. Notably, mutations in the *lptD* gene appeared consistently across resistant strains, implying its importance in resistance to Oct-TriA₁. We then conduct further investigations into the role of *lptD*, *miaA* and *ompC* mutations through allelic replacement studies, demonstrating their effect on Oct-TriA₁ and other antibiotics' minimum inhibitory concentrations (MICs), as well as their fitness costs.

2. Results

2.1. Standard SAGE medium fails to generate resistance to polymyxin B

To begin testing the ability of SAGE to generate resistance to lipopeptides, we attempted to evolve resistance to PolB in *Escherichia coli* K-12 substr. BW25113. However, we repeatedly failed to evolve resistance greater than 4-fold the initial value of 0.25 µg/mL. At low PolB concentrations ([PolB]_{max} = 1.25 µg/mL, 5x MIC), cells quickly covered the plate and on isolation gave MICs that were 2x-4x that of the wildtype strain. However, the susceptibility of these mutants quickly reverted to

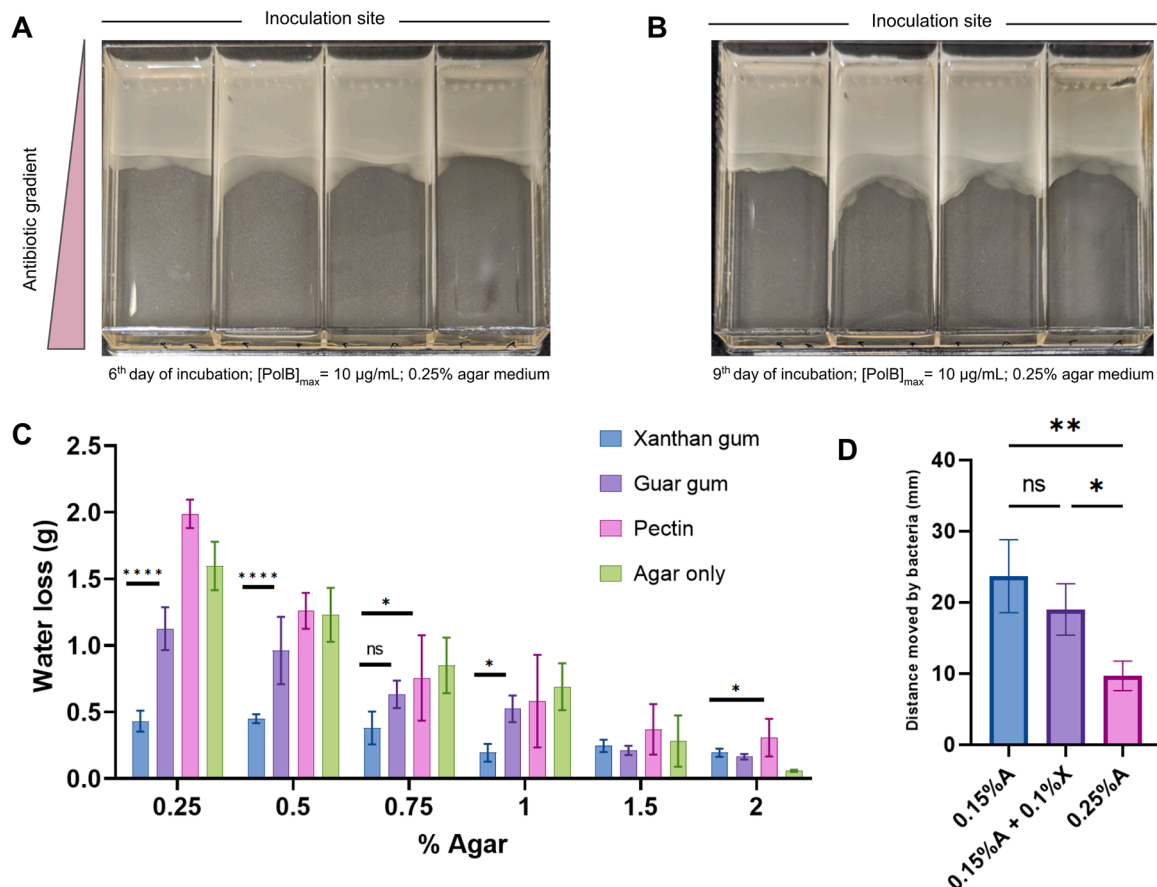


Fig. 1. Syneresis limits SAGE. (A) Cells in 0.25 % agar-based PolB SAGE plates ([PolB]_{max} = 10 µg/mL) remain stationary ~30 mm from the inoculation site. (B) Further incubation results in only small movements of the bacterial front. (C) Xanthan gum outperforms all other additives tested for syneresis-resistance across a range of agar strengths (n = 5). (D) Distance moved by bacteria in 0.15 % agar medium (0.15 %A), 0.15 % agar + 0.1 % xanthan gum medium (0.15 %A + 0.1 %X), and 0.25 % agar medium (0.25 %A). Bacteria traverse significantly higher distances in the 0.15 %A + 0.1 %X medium compared to the 0.25 %A (n = 3). * p < 0.05, ** p < 0.01, *** p < 0.001, **** p < 0.0001, one-way ANOVA with Fisher's LSD test. Error bars represent SD.

wildtype (WT) levels upon subculturing in antibiotic-free media (data not shown), a feature consistent with the heteroresistance often observed with polymyxins like PolB and colistin (Hjort et al., 2016; Andersson et al., 2019; Liao et al., 2020). Growth in plates with a higher $[\text{PolB}]_{\text{max}}$ (10 $\mu\text{g}/\text{mL}$, 40x MIC) failed to reach the end of the plates (Figs. 1A, 1B). This behaviour is consistent with other ALE platforms, and PolB is known to be difficult to evolve resistance to via ALE (Trimble et al., 2016).

SAGE evolutions rely on the ability of bacteria to move through the antibiotic gradients set up in soft-agar (0.25 % agar) (Ghaddar et al., 2018). During incubation, syneresis increases the effective agar concentration, reducing bacterial motility. We noticed that the bacterial front in PolB SAGE plates incubated for more than a week scarcely moved (Fig. 1A, 1B), and hypothesized that syneresis may be hindering the emergence of chromosomal mutations that confer stable PolB resistance. In line with this, a previous study reported that resistance to PolB in *E. coli* did not evolve for ~6 days (in a liquid evolution platform), after which a rapid increase in resistance was seen (Yoshida et al., 2017). The authors proposed a two-step trajectory of resistance where heteroresistant bacterial populations leverage non-genetic mechanisms to withstand PolB stress at low concentrations, accessing stable chromosomal mutations only when the antibiotic concentrations increased (Yoshida et al., 2017). We thus set out to develop a SAGE medium more suitable for prolonged experiments.

2.2. Xanthan gum supplementation reduces syneresis in agar hydrogels

Polysaccharides like pectin, guar gum, and xanthan gum are able to form hydrogen bonds with water molecules, and are widely used as thickening agents in the food industry (Sánchez et al., 1995; Einhorn-Stoll, 2018). We hypothesized that the addition of these water-binding agents to agar gels may help slow down the syneresis-driven remodeling of the agar matrix by resisting expulsion of water. We first confirmed that *E. coli* cannot utilize these polysaccharides as a carbon source (Supplementary Figure 1), then evaluated their effect on the syneretic properties of agar gels. Each agent was separately added at 0.25 % to agar strengths ranging from 0.25 % to 2 % (all percentages are in w/v), and the extent of syneresis was evaluated via a modification of the method described by Banerjee et al. (Banerjee and Bhattacharya, 2011). Gels supplemented with xanthan gum achieved the highest reduction in water loss at all agar strengths tested (Fig. 1C). While not a gelling agent itself, xanthan gum could replace a proportion of the agar while maintaining gel cohesion and limiting syneresis (Supplementary Figure 2), though the medium became viscous at higher xanthan gum strengths.

Next, we tested the effect of addition of xanthan gum on bacterial motility in the SAGE medium. Addition of 0.1 % xanthan gum to 0.15 % agar had no statistically-significant effect on bacterial motility when compared to 0.15 % agar alone, and both offered significant improvements in motility compared to the 0.25 % agar medium (Fig. 1D, Supplementary Figure 3).

2.3. Supplementation with xanthan gum enhanced the evolution of polymyxin B resistance

Moving forward, we opted to use a mixture of 0.2 % xanthan gum and 0.15 % agar (referred to from here on as XAM), a ratio which provided a balance of low viscosity in liquid state and high stability in the gel state, in place of the conventional 0.25 % agar base used in SAGE. We found no difference between diffusion rates of malachite green in 0.25 % agar and XAM (Supplementary Figure 3B), indicating that diffusion rates of antibiotics in XAM should be similar to that in the conventional medium.

To test the performance of the medium in SAGE, we set up a PolB SAGE plate with XAM ($[\text{PolB}]_{\text{max}}$ in SAGE = 10 $\mu\text{g}/\text{mL}$, 40x MIC). We were able to generate stable PolB resistant mutants within 4 days in 2/4

SAGE lanes (MIC: 16 $\mu\text{g}/\text{mL}$, Fig. 2A). We suspect that the increase in bacterial movement speed in xanthan gum-supplemented media (Fig. 1D) reduced the time required for evolution in XAM-SAGE plates by allowing bacteria to reach PolB concentration that selects for stable genomic mutations earlier. By the time cells reached this concentration in the conventional medium, the medium may have already been too dry to allow movement.

2.4. Evolution of resistance to Oct-TriA₁

We next sought to evolve resistance to Oct-TriA₁ in XAM. We set up two SAGE lanes in parallel ($[\text{Oct-TriA}_1]_{\text{max}} = 40 \mu\text{g}/\text{mL}$, 10x MIC), one with the conventional 0.25 % agar medium, and the other with XAM. We followed the evolution of resistance by measuring the maximum distance moved by the bacterial fronts every 24 h (Fig. 2B). Bacteria moved slowly through the 0.25 % agar medium, traversing only about 60 % of the lane (~50 mm) by the end of 25th day and remaining stationary for 3 additional days before the experiment was stopped (Fig. 2B). The small distances moved and thinning agar gel made sampling from this medium beyond 7 days challenging. In contrast, bacteria in the XAM lane moved large distances after breaking free from the initial inhibitory Oct-TriA₁ concentration (Day 7), covering the entire lane by the end of day 17 (Fig. 2B). The XAM gel also appeared to have retained significantly more water than the agar-based gel at the end of the experiment (data not shown). Samples were collected whenever significant bacterial movement was detected since cells that continued moving towards higher concentration of the antibiotic may have acquired adaptive mutations against Oct-TriA₁. We sampled 20 μL of gel out of the plates every sampling. While sampling may reduce the population size of a mutant on the plate, it is unlikely to alter the evolutionary trajectory. We previously showed that varying population sizes in SAGE plates containing nitrofurantoin did not change the adaptation rate (Chowdhury and Findlay, 2023). We tested the MIC of samples A26, A30, A37, A51, XAM34, XAM45, XAM56 and XAM CM ('A' and 'XAM' in the sample IDs denote samplings from 0.25 % agar lane and XAM respectively, and the numbers denote the distance in millimeters from the inoculation zone to where cells were sampled; CM = cells extracted from the end of lane, ~75 mm) (Table 1). The MIC of A26 and XAM34, both from the 9th day of incubation, showed that resistance emerged early, and appeared to remain constant throughout the rest of the experiment (Table 1). This could partly be due to partial flattening of the Oct-TriA₁ gradient via diffusion, presenting an antibiotic challenge that allowed bacteria to evolve resistance to a level which remained sufficient for the rest of the plate. Also, since standard MIC assays are based on 2-fold dilution steps, small increases in MIC that might have occurred after the initial increase may not have been resolved via our MIC assays. Overall, mutants from the 0.25 % agar-based medium exhibited up to 4x increase in MIC, compared to an 8x increase in XAM (Table 1).

Next, we compared the fitness of the early and endpoint Oct-TriA₁ mutants to that of the WT parent strain (Fig. 2C). The WT *E. coli* used for generating mutants from the 0.25 % agar lane was pre-adapted to this SAGE medium as previously described (Ghaddar et al., 2018). To account for any changes in fitness due to adaptation to XAM, we also passaged the WT strain through antibiotic-free XAM 3 times to produce a XAM-adapted WT strain (Materials and Methods). All evolved mutants showed longer lag times (though differences with A51 did not reach statistical significance) and lower growth rates, yields and AUCs (area under the growth curves), indicating that Oct-TriA₁ resistance imposed a large fitness cost (Fig. 2C). In general, the XAM-generated mutants showed larger fitness deficits, even though the fitness of the XAM-adapted WT was comparable to the WT in every metric measured. Interestingly, the XAM CM strain showed a clear diauxic growth pattern (Supplementary Figure 4). While a delayed release of glucose from degradation of xanthan gum could affect growth during our long evolution experiment, the stability of xanthan gum makes it unlikely for significant amounts of monomers to be released in the medium at 37 °C

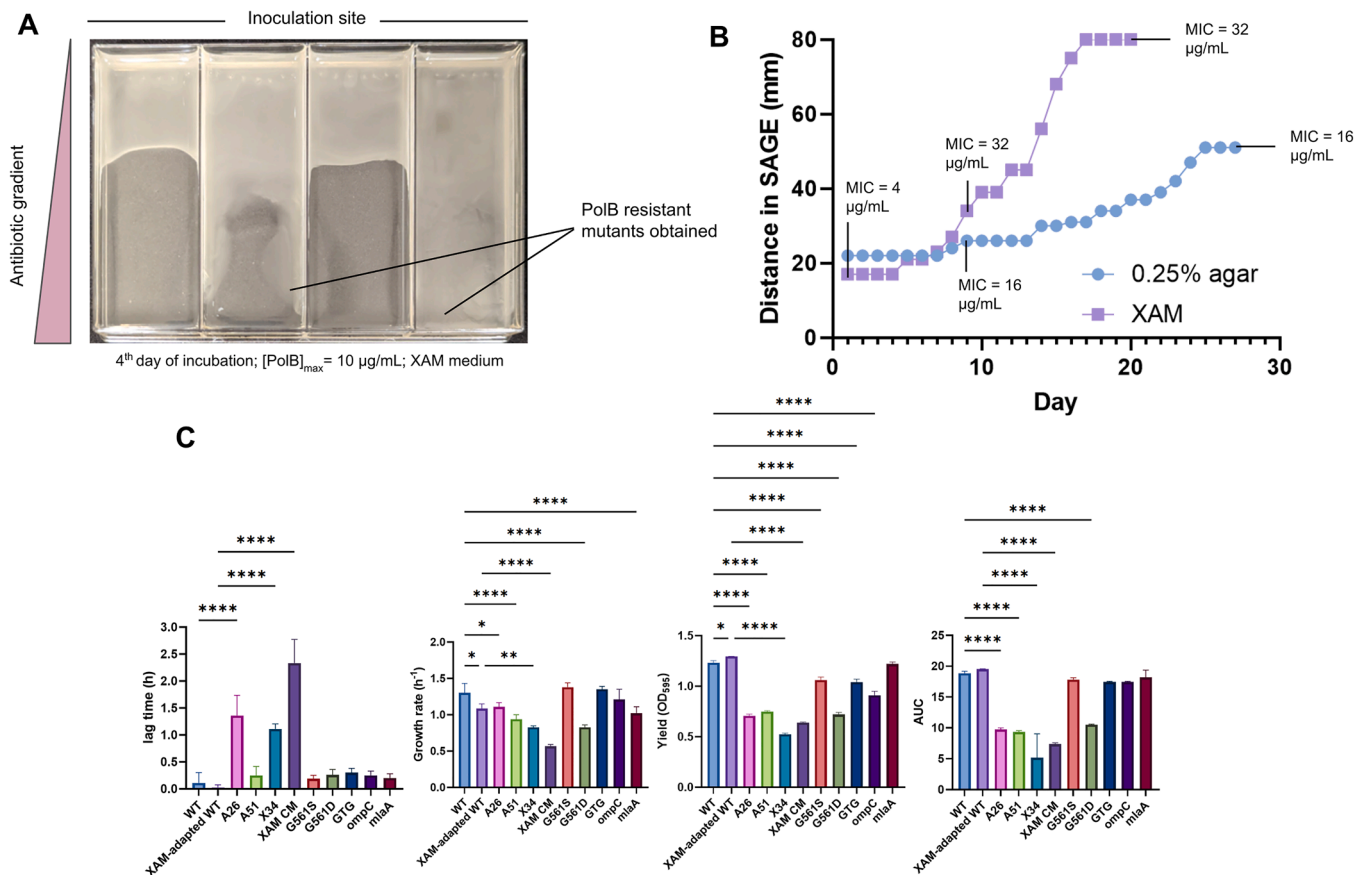


Fig. 2. Evolution of antibiotic resistance. (A) Resistance to PolB emerged in 2 out of the 4 replicates in SAGE with XAM ([PolB]_{max} = 10 μg/mL). (B) Distance moved by bacteria swimming through agar or XAM SAGE plates loaded with Oct-TriA₁ at a max concentration of 40 μg/mL. Bacteria moved farther and faster in XAM. MIC of samples from several time points are labelled, with bacteria in XAM achieving a higher MIC (full list of MICs in Table 1). (C) Oct-TriA₁ mutants are fitness impaired (n = 3). * p < 0.05, ** p < 0.01, *** p < 0.001, **** p < 0.0001, one-way ANOVA with Bonferroni correction. For statistical comparisons, WT values were compared with XAM-adapted WT, A26, A51, G561S, G561D, GTG, ompC and mlaA, and XAM-adapted WT values were compared with XAM34 and XAM CM. Among these comparisons, only statistically significant differences are indicated by asterisks. Error bars represent SD. Results obtained from 3 to 9 replicates.

Table 1
Details of Oct-TriA₁ mutants sampled from SAGE.

Strain ID	Media in SAGE lane	Sampling day	Oct-TriA ₁ MIC (μg/mL)
WT	-	-	4
XAM-adapted	XAM	-	4
WT	-	-	4
A26	0.25 % agar	9	16
A30	0.25 % agar	14	16
A37	0.25 % agar	21	16
A51	0.25 % agar	27	16
XAM34	XAM	9	32
XAM45	XAM	12	32
XAM56	XAM	14	32
XAM CM	XAM	20	32

since it remains stable over multiple years at temperatures above 70 °C and was insufficient to maintain bacterial growth (Seright and Henrici, 1990; Jouenne, 2020) (Supplementary Figure 1). This strain harbored a deletion in the *nuo* operon, which codes for a NADH/ubiquinone oxidoreductase that shuttles electrons from NADH into the electron transport chain (Prüss et al., 1994; Van den Bergh et al., 2022). When cells grow in the presence of glucose, they excrete acetate (Shimada and Tanaka, 2016). As cells deplete glucose from media, they switch to uptaking acetate (Shimada et al., 2021), shifting from glycolysis to TCA cycle and gluconeogenesis (Shimada and Tanaka, 2016). In *nuo* mutants, high NADH/NAD⁺ ratios inhibit enzymes involved in the TCA cycle,

drastically slowing growth and potentially giving rise to the diauxic growth pattern we observed (Prüss et al., 1994; Shimada et al., 2021). However, what causes subsequent resumption of growth during diauxia is unclear (Chu and Barnes, 2016; Salvy and Hatzimanikatis, 2021).

2.5. Genetic analysis of Oct-TriA₁-resistant mutants

We whole genome sequenced four strains from our SAGE evolution experiments: A26, A51, XAM34 and XAM CM (Fig. 3). Mutations in A26 and XAM CM were not complete subsets of A51 and XAM CM respectively, showing that different clones were selected along the SAGE lanes during these samplings. This suggests mutants that appeared early did not maintain their selective advantage, and other mutants that gained an advantage at different time points (and hence, at different states of the gradient) surpassed the earlier mutants. XAM34 had an MIC eight times that of the wildtype *E. coli* BW25113 and had eight mutations: three non-synonymous, three intergenic, and two frameshift insertions (Table 1, Fig. 3). XAM CM, drawn from later in the same SAGE plate, had the same MIC and ten mutations: four non-synonymous, two intergenic, three frameshift insertions, and one frameshift deletion. Two of these were identical: a five-base deletion in *yddW* and a E26K mutation in *rpoD*. A26 had two nonsynonymous mutations and the same five-base deletion in *yddW*, while A51 had four non-synonymous mutations, one intergenic mutation, one insertion, and three frameshift mutations (including the five-base deletion in *yddW*).

To separate possible resistance mutations from those that might be associated with adaptation to the ALE conditions, we sequenced the XG-

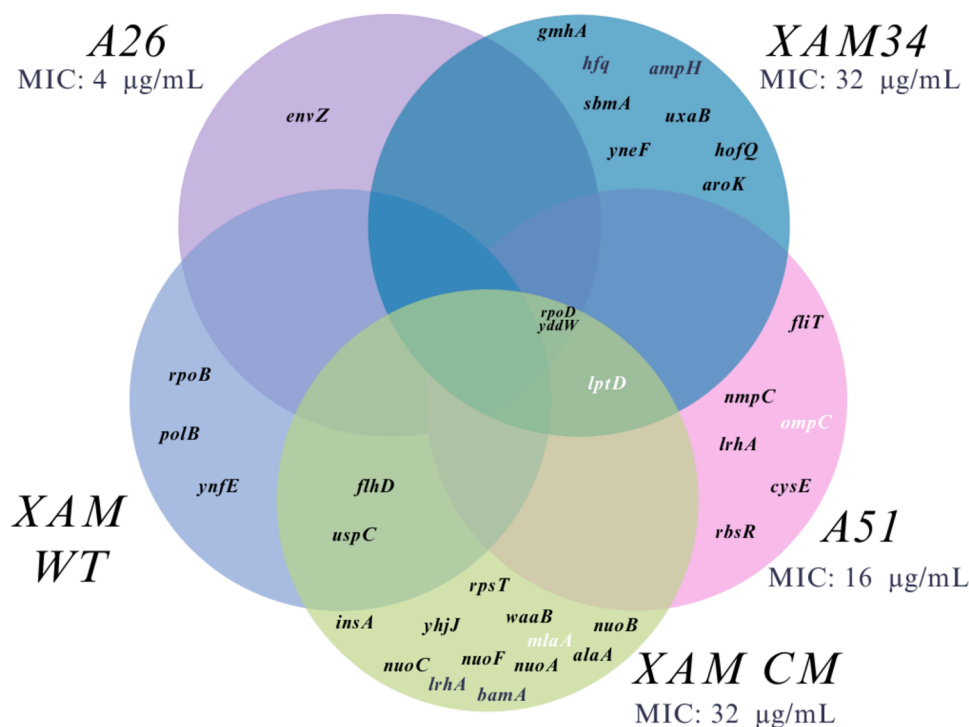


Fig. 3. Mutations identified in the evolved strains. A26 and A51 represent mutations observed in cells isolated at 26 mm and 51 mm in agar media; XAM 34 and XAM CM cells isolated at 34 mm and 75 mm, respectively in xanthan gum-supplemented media. The highlighted mutations were selected for allelic exchange.

adapted WT for comparison with the XAM-generated Oct-TriA₁ mutants. Only one mutation overlapped with the antibiotic-exposed samples; an intergenic mutation in *flhD* ← / → *uspC* that was also found in XAM CM. The XAM evolved strain carried a G→T mutation in -261/-519 while the XAM CM carried a C→A in -263/+ 44. FlhD is involved in flagellar type II transcription activation and UspC is a universal stress protein. Changes in *flhD* expression may alter swimming speed, enhancing movement through the soft agar plates (Barker et al., 2004; Wang and Wood, 2011; Lee and Park, 2013). Other mutations observed were in *rpoB*, *ynfE* and *polB* genes, genes not mutated in any of the antibiotic-exposed strains.

All strains with MICs higher than the wild type carried a single nucleotide polymorphism in *lptD*, creating LptD G561S (A51, XAM 34) or G561D (XAM CM). This was also the only gene to contain two mutations, with A51 having a further (GTG)₃→2 deletion in nucleotides 705-707. LptD is an integral component of the Lpt complex, which is essential for the assembly and transport of LPS to the outer membrane of Gram-negative bacteria (Chng et al., 2010). Mutations were also observed in two other genes linked to LPS biosynthesis: X34 contained a SNP in *gmhA*, which encodes a phosphoheptose isomerase that produces the D-glycero-D-manno-heptose 7-phosphate found in the core of LPS (Taylor et al., 2008), while XAM CM contained a frameshift mutation in *waaB*, which encodes a galactosyltransferase that appends galactose to that core (Qian et al., 2014). Similar to polymyxin B (Trimble et al., 2016), tridecaptin A₁ engages with LPS in the outer membrane to facilitate uptake into the intermembrane space and access its target (Cochrane et al., 2016), and these mutations strongly suggest that tridecaptin resistance is conferred by alterations in LPS structure.

Three other mutations had clear ties to the bacterial outer membrane: *mlaA* directly regulates outer membrane composition and was heavily truncated in XAM CM (MlaA W59 *), while the porin gene *ompC* is implicated in both maintenance of outer membrane integrity and drug uptake (Chong et al., 2015; Choi and Lee, 2019). Notably, *OmpC* was altered both directly through a nonsynonymous *ompC* SNP (*OmpC* N47S) in A51 and indirectly through a nonsynonymous SNP in the *omp* regulator *envZ* (*EnvZ* R253S) in A26. A SNP was also observed in *bamA*

(*BamA* L501Q; XAM CM), part of the BAM complex (Lehman and Grabowicz, 2019). *BamA* is responsible for inserting β-barrel proteins into the OM (Lehman and Grabowicz, 2019). Mutations in *bamA* have been related to resistance to drugs targeting this OM protein (Hart et al., 2019; Luther et al., 2019; Kaur et al., 2021). In the case of darobactin, resistance mutations in *bamA* also result in loss of virulence (Huang et al., 2019).

Gene ontology enrichment analysis mapped the remaining mutations to several key pathways, including those related to respiratory electron transport mechanisms (Supplementary Table 1). This suggests adaptive changes in electron transport and ATP synthesis, in addition to alterations in outer membrane assembly and biosynthesis.

2.6. Allelic exchange in genes involved in phospholipid transport and outer membrane assembly confirmed their involvement in resistance to Oct-TriA₁

To investigate the effect of mutations in genes associated with phospholipid transport, we introduced the observed mutations in *lptD* into *E. coli* BW25113 via allelic exchange. This was carried out using CRISPR-Cas9/λ-Red assisted recombineering as previously described (Reisch and Prather, 2015, 2017). Concurrently, knockouts in *ompC* and *mlaA* were obtained from the Keio collection (Baba et al., 2006). The effect of these alterations was assessed via MIC assays, revealing that all five alterations increased the ancestral strain's MIC against Oct-TriA₁ two-fold (Supplementary Figure 5).

Other cationic non-ribosomal peptides (CNRP) like Polymyxin and Brevicidine (Li et al., 2018b) have a similar uptake mechanism (Zhao et al., 2023) (Manioglu et al., 2022). Specifically, brevicidine also targets components in the inner membrane, namely phosphatidylglycerol and cardiolipin. Given the similarities in their mechanisms of action, the mutations related to LPS biosynthesis and transport conferring Oct-TriA₁ resistance may also result in cross-resistance to brevicidine. Although we did not observe cross-resistance to Polymyxin B in our study (Supplementary Figure 5), it is important to consider broader implications of cross-resistance in antimicrobial strategy development.

Exploring these targets that haven't been extensively used in the clinic could provide an advantage in delaying the appearance of resistance.

The effect of the mutations on fitness was more variable. None of the mutations altered lag times during growth in MHB, but significant deviations were observed in both growth rates and max OD (Fig. 2C). The effect of the LptD mutations on fitness varied by both site and type of mutation. Despite halving susceptibility towards OctTriA1, the lost GTG repeat had no effect on bacterial fitness, while the LptD G561D mutation was much more detrimental than the LptD G561S mutation. As no single mutation increased resistance or impaired fitness to the levels observed in XAM CM, a combination of costly mutations appears to be required for high-level resistance.

3. Discussion

In this study we demonstrate the first *de novo* evolution of resistance to Oct-TriA₁, with the effect of putative resistance-conferring mutations confirmed through allelic exchange. Further, we have improved the SAGE system through the incorporation of the thickening agent xanthan gum, extending the potential duration of experiments from a week to a month and enhancing selection rates. This modified system was also much more effective at selecting mutants resistant to polymyxin B, an antibiotic that is often difficult to target with other ALE systems.

In line with resistance to other D-amino acid-containing non-ribosomal peptides (Li et al., 2018a), resistance in the native producers of tridecaptins is mediated via hydrolytic D-stereospecific peptidases (Bann et al., 2021). In contrast, the mutations we have observed are largely in genes coding for LPS biosynthesis and outer membrane homeostasis. These pathways are essential to bacterial growth, as well as interactions with the immune system, nutrient acquisition, and toxin susceptibility (Liu et al., 2012; Phan and Ferenci, 2017; Simpson and Trent, 2019). As a result, it is unsurprising that the resistant strains we generated had significantly impaired fitness (Fig. 2C). Similar results have been observed with other membrane-interacting antibiotics, like the polymyxins. In many pathogens mutations that confer colistin resistance significantly impairs fitness and/or virulence (Wang et al., 2022), though acquisition of the plasmids encoding colistin resistance factor *mcr-1* has a much smaller impact (Tietgen et al., 2018).

The factors that underpin widespread, high-level resistance are not fully understood. When evaluating evolution potential there has been a strong tendency to focus on the rate by which resistance emerges, either through mutation rate studies or ALE (Martinez and Baquero, 2000; Cirz et al., 2005; Ling et al., 2015; Cochrane et al., 2016; Sommer et al., 2017; Stokes et al., 2020; Martin et al., 2020). This work suggests that the nature of the mutations should also be taken into account. Each of the mutations in *lptD*, *mfaA*, and *ompC* altered the octyl-tridecaptin A₁ MIC two-fold, with little overlap between strains (Fig. 3, S4). Given the overall change in susceptibility following SAGE was 8-fold, high-level resistance likely resulted from a combination of multiple mutations rather than from any single mutation. SAGE is well-suited to the serial acquisition of small-impact mutations (Ghaddar et al., 2018), potentially explaining why it was successful when attempts to evolve resistance via serial passage through liquid culture failed (Cochrane et al., 2016).

Xanthan gum was able to significantly reduce synaeresis and allow SAGE experiments to extend beyond their initial limit of 7–10 days, and this media may have utility outside ALE. Synaeresis causes loss of growth-promoting properties of media when cultivating slow-growing bacteria and fungus (Laserna et al., 1981; Divoux et al., 2015; Savinova et al., 2023). Addition of a water-binding agent like xanthan gum may preserve these properties, allowing extension of those experiments as well.

Against the rising prevalence of antibiotic resistance, “evolution-proof” or “resistance-proof” are very appealing targets (Bell and MacLean, 2018; Upadhyay et al., 2023). Their discovery could greatly alleviate the growing AMR crisis, carving a path forward for the use of antibiotics for decades to come. However, since the discovery of sulfa

drugs hundreds of antibiotics have entered clinical use, with pathogens evolving resistance to each and every one of them (Bell and MacLean, 2018). This work underscores the genetic flexibility of bacteria, and highlights the need for stringent evolution studies during the development and discovery of new antibiotics. If resistance is to emerge, we would do well to study it *in vitro* before its appearance in pathogens.

4. Materials and methods

4.1. Bacterial strain and growth conditions

E. coli K-12 substr. BW25113 and all subsequent resistant mutants were grown in cation-adjusted Mueller Hinton Broth (MHB 2) media at 37 °C. Liquid cultures were shaken at 250 rpm, while agar cultures were grown in a static incubator.

4.2. Oct-TriA₁ synthesis

Oct-TriA₁ synthesis was performed as described by Cochrane et al. (2014b), with the following modifications. Briefly, in a manual peptide synthesizer 120.5 mg of Wang resin pre-loaded with Fmoc-Alanine at a loading of 0.6 mmol/g was swelled in dimethylformamide (DMF). The protecting group was cleaved with two twenty-minute treatments of 4:1 DMF:4-methylpiperidine. The beads were then washed three times with DMF, once with dichloromethane (DCM), then one final time with DMF. The next residue in the series was then added in 3x excess, alongside HATU (3x excess) and diisopropylethylamine (DIPEA) (8x excess). Coupling was carried out for one hour, at which point the beads were washed as above and the Fmoc protecting group once more cleaved. This cycle was repeated for each of the peptides, with Fmoc-Glu(OtBu)-OH, Fmoc-D-Ser(OtBu)-OH, Fmoc-Dab(Boc)-OH, and Fmoc-D-Dab(Boc)-OH used for the residues with reactive side chains. The complete peptide was cleaved from the resin with a 95:2.5:2.5 solution of trifluoroacetic acid (TFA):deionized water:triisopropylsilane for 2 hours. The cleavage solvent was removed on a rotary evaporator, and the crude material was triturated three times with diethyl ether. The solid residue was then purified to homogeneity on an Agilent 1100 preparative HPLC system, using an XBridge BEH C18 OBD prep column (5 µm, 25 × 250 mm) and the following water/acetonitrile gradient system.

Time	Acetonitrile (%)
0	5
1	5
3	20
23	55
31	95
36	95

Peaks eluting around 13.2 min across multiple runs were pooled, and the identity of the peptide was confirmed via high resolution mass spectrometry on an Orbitrap LTQ Velos.

4.3. SAGE evolutions

SAGE plates were prepared and inoculated as described previously (Ghaddar et al., 2018). For SAGE plates made with XAM, MH media + 0.15 % agar was first stirred in a flask on a hot plate and stirrer on high for 5–10 minutes. 0.2 % xanthan gum was then slowly added to the stirring liquid and the mixture was allowed to stir for 2–3 minutes before autoclaving. This medium was melted on demand prior to use in SAGE plates. We checked on the plates every day to measure distance moved by the bacterial front, and we extracted bacteria only when the bacterial front moved significantly from the previous measurement. Bacteria were extracted from the point where they moved the farthest from the inoculation site. Cells were extracted from SAGE plates by pipetting up 20 µL of the gel and transferring it into 5 mL MH media for culturing.

Overnight growth was streaked on MH plates and single colonies were used to prepare glycerol stocks.

4.4. MIC assays

MICs were determined via broth microdilution, following CLSI guidelines (CLSI, 2018). Briefly, antibiotics were serially diluted in 96-well plates and mixed with bacteria at a final concentration of 5×10^5 CFU/mL. Plates were incubated at 37 °C without shaking for 16–20 h, and the MIC was recorded as the lowest concentration that visibly inhibited growth.

4.5. Synaeresis tests

Water loss from different gel mixtures was measured as described by Banerjee and Bhattacharya (2011) with the following modifications. Agar concentrations ranging from 0.2 % to 2 % were first stirred in a flask on a hot plate for 5–10 minutes. 0.25 % xanthan gum, guar gum or pectin was then slowly added to the stirring liquid, which was allowed to stir for 2–3 minutes. Flasks were transferred to a 37 °C shaker and shaken overnight at 250 rpm to produce a smooth, homogenous mixture. The flasks were then autoclaved, and 20 mL of each liquid was transferred to 50 mL centrifuge tubes. Tubes were allowed to cool at room temperature, then stored at 4 °C overnight. Initial masses of the tubes were recorded (~30 g on average) before centrifugation at 1000 rpm for 30 minutes at 25 °C. Centrifugation broke the gel structure, making it difficult to decant water out of the tubes without losing gel mass. To extract the free liquid tubes were instead left upright with their caps open and a folded filter paper was used to wick away the water over 30 minutes. The filter papers were then carefully removed to minimize the loss of gel mass, and the final tube masses were recorded. Water loss was calculated as the difference between the initial and the final masses of the tubes.

4.6. Bacterial motility tests

Bacterial migration speeds on different gel compositions were measured as described by Croze et al. (2011). The media were prepared as described above. 30 mL of each mixture was then poured in separate petri dishes, and the plates were left to set overnight at room temperature. 2 µL of overnight bacterial culture was placed on the center of each petri dish, and the inoculum was allowed to dry/absorb for an hour. 9 mL of mineral oil was overlaid on each plate, and all plates were then incubated at 37 °C without shaking, lid side up. The diameter of growth was measured 6 h post incubation.

4.7. Generation of the XAM-adapted WT strain

12 mL of antibiotic-free XAM was poured in a SAGE lane and allowed to cool and solidify. 50 µL of overnight WT bacterial culture was then inoculated on one side and the inoculum was allowed to dry/absorb for 30 minutes. 2.5 mL of mineral oil was overlaid on the gel, and the plate was incubated at 37 °C. The next day, cells were extracted from the end of the lane as described above, then grown overnight. These cells were used to inoculate a second antibiotic-free XAM lane and the whole process was repeated. Following three consecutive passes, cells were streaked on agar, and a single colony was designated as the XAM-adapted WT strain.

4.8. Fitness measurements

1 µL of overnight bacterial culture was added to 99 µL of MH broth in 96 well plates. Lids were treated with 0.05 % Triton X-100 in 20 % ethanol to reduce fogging (Brewster, 2003). Absorbance readings (595 nm) were recorded using a plate reader at 5 min intervals for 24 h (Tecan Sunrise). Area under the growth curves were calculated in

GraphPad Prism. All other metrics were generated using Dashing Growth Curves (Reiter and Vorholt, 2024).

4.9. WGS and variant calling

Whole genomes were extracted using a bacterial genomic DNA extraction kit following the manufacturer's instructions (Bio Basic Inc, Cat: BS624). Whole genome sequencing was performed at SeqCenter using the Illumina NovaSeq X Plus sequencer, which generated 2×151 bp paired-end reads. The Breseq v0.37.1 pipeline was used for variant calling with bowtie2 v2.4.5 and R v4.2.2 (Barrick et al., 2014).

4.10. Gene ontology enrichment analysis

Mutations observed in all of the evolved strains were analyzed for enrichment of gene ontology groups using the ShiniGO package v0.741 (Ge et al., 2020). The p-value cut-off for the False Discovery Rate (FDR) was set to 0.05 against *E. coli* MG1655, a K12 strain. Several previously reported differences between MG1655 and BW25113 were identified and excluded from the analysis (Grenier et al., 2014); most notably deletion of the *araBAD* and *rhaDAB* operons, replacement of a section of the *lacZ* gene with four *rrnB* terminators, and a frameshift mutation in *hsdR* that causes a premature stop codon.

4.11. Allelic exchange mutant generation

Allelic exchange of the selected mutated genes was carried out using the no-SCAR (Scarless Cas9 assisted recombineering) method, as previously described (Reisch and Prather, 2015, 2017). In short, retargeting of the pKDsgRNA plasmid was constructed for the *lptD* gene region of interest through CPEC cloning in a way that the mutation would disrupt the PAM site or the 12 bp seed region. Cas9 counterselection was achieved by sequentially transforming pCas9cr4 and the retargeted pKDsgRNA and electroporating dsDNA containing the desired mutation. Following induction of λ-Red and Cas9, the successful mutants were verified and the plasmids were cured of the plasmids to render them susceptible to chloramphenicol and spectinomycin.

4.12. Keio collection strains Kan cassette curing

Keio collection strains were cured of the kanamycin resistance cassette through FLP-recombinase-mediated recombination, using the pCP20 plasmid as previously described (Datsenko and Wanner, 2000; Baba et al., 2006). Subsequent curing of temperature sensitive pCP20 plasmid yielded Kan^S, Amp^S for MIC determination.

5. Strains

Strain	Genotype	Reference
<i>E. coli</i> BW25113	$\Delta(\text{araD-araB})567 \Delta(\text{rhaD-rhaB})568 \Delta\text{lacZ4787} (::\text{rrnB}-3) \text{hsdR514 rph-1}$	(Baba et al., 2006)
<i>E. coli</i> BW25113 <i>lptD</i> G561S	$\Delta(\text{araD-araB})567 \Delta(\text{rhaD-rhaB})568 \Delta\text{lacZ4787} (::\text{rrnB}-3) \text{hsdR514 rph-1 lptDG561S}$	This study
<i>E. coli</i> BW25113 <i>lptD</i> G61D	$\Delta(\text{araD-araB})567 \Delta(\text{rhaD-rhaB})568 \Delta\text{lacZ4787} (::\text{rrnB}-3) \text{hsdR514 rph-1 lptDG561D}$	This study
<i>E. coli</i> BW25113 <i>lptD</i> (GTG)3→2	$\Delta(\text{araD-araB})567 \Delta(\text{rhaD-rhaB})568 \Delta\text{lacZ4787} (::\text{rrnB}-3) \text{hsdR514 rph-1} \Delta\text{lptD}(\text{GTG})3 \rightarrow 2$	This study
<i>E. coli</i> BW25113mlaA (vacJ) JW2343-1	F-, $\Delta(\text{araD-araB})567, \Delta\text{lacZ4787} (::\text{rrnB}-3), \lambda-, \Delta\text{mlaA754}::\text{kan}, \text{rph-1}, \Delta(\text{rhaD-rhaB})568, \text{hsdR514}$	(Baba et al., 2006)
<i>E. coli</i> BW25113 ΔompC JW2203-1	F-, $\Delta(\text{araD-araB})567, \Delta\text{lacZ4787} (::\text{rrnB}-3), \lambda-, \Delta\text{ompC768}::\text{kan}, \text{rph-1}, \Delta(\text{rhaD-rhaB})568, \text{hsdR514}$	(Baba et al., 2006)

Declaration of Generative AI and AI-assisted technologies in the writing process

During the preparation of this work the authors used ChatGPT Plus (OpenAI, GPT-4) to generate alternative phrasings for complex sentences. These alternative sentences were then spliced and edited as needed, and the authors take full responsibility for the content of the published article.

CRedit authorship contribution statement

Farhan R. Chowdhury: Writing – original draft, Validation, Methodology, Investigation. **Laura Dominguez Mercado:** Writing – original draft, Validation, Investigation. **Katya Karitonov:** Writing – review & editing, Investigation. **Brandon L. Findlay:** Writing – review & editing, Supervision, Methodology, Investigation, Funding acquisition, Conceptualization.

Declaration of Competing Interest

The authors declare that they have no known competing financial interests or personal relationships that could have appeared to influence the work reported in this paper.

Acknowledgments

This work was funded by the Fonds de recherche du Québec – Santé (FRQS) (269182). FRC and LDM are supported by the Fonds de recherche du Québec – Santé (FRQS) (B2X). KK was supported by the Natural Sciences and Engineering Research Council of Canada (NSERC) (USRA). We thank Rami Antoun and Madeleine Woisin for their help with Oct-TriA₁ synthesis.

Appendix A. Supporting information

Supplementary data associated with this article can be found in the online version at [doi:10.1016/j.micres.2025.128056](https://doi.org/10.1016/j.micres.2025.128056).

Data Availability

WGS data is available under the NCBI sequence Read Archive BioProject: PRJNA1131392; BioSample accession numbers SRR29693652, SRR29693651, SRR29693650, SRR29693649, SRR29693648 and SRR29693647. <https://www.ncbi.nlm.nih.gov/bioproject/PRJNA1131392>.

References

- Andersson, D.I., Nicoloff, H., Hjort, K., 2019. Mechanisms and clinical relevance of bacterial heteroresistance. *Nat. Rev. Microbiol.* 17, 479–496.
- Baba, T., Ara, T., Hasegawa, M., Takai, Y., Okumura, Y., Baba, M., et al., 2006. Construction of *Escherichia coli* K-12 in-frame, single-gene knockout mutants: the Keio collection. *Mol. Syst. Biol.* 2, 2006.0008.
- Ballantine, R.D., McCallion, C.E., Nassour, E., Tokajian, S., Cochrane, S.A., 2019. Tridecaptin-inspired antimicrobial peptides with activity against multidrug-resistant Gram-negative bacteria. *MedChemComm* 10, 484–487.
- Banerjee, S., Bhattacharya, S., 2011. Compressive textural attributes, opacity and syneresis of gels prepared from gellan, agar and their mixtures. *J. Food Eng.* 102, 287–292.
- Bann, S.J., Ballantine, R.D., Cochrane, S.A., 2021. The tridecaptins: non-ribosomal peptides that selectively target Gram-negative bacteria. *RSC Med Chem.* 12, 538–551.
- Barker, C.S., Prüß, B.M., Matsumura, P., 2004. Increased Motility of *Escherichia coli* by Insertion Sequence Element Integration into the Regulatory Region of the flhD Operon. *J. Bacteriol.* 186, 7529–7537.
- Barrick, J.E., Colburn, G., Deatherage, D.E., Traverse, C.C., Strand, M.D., Borges, J.J., et al., 2014. Identifying structural variation in haploid microbial genomes from short-read resequencing data using breseq. *BMC Genom.* 15, 1039.
- Bell, G., MacLean, C., 2018. The search for ‘evolution-proof’ antibiotics. *Trends Microbiol.* 26, 471–483.

- Bonomo, R.A., Perez, F., Hujer, A.M., Hujer, K.M., Vila, A.J., 2024. The real crisis in antimicrobial resistance: failure to anticipate and respond. *Clin. Infect. Dis.* cjad758.
- Brewster, J.D., 2003. A simple micro-growth assay for enumerating bacteria. *J. Microbiol Methods* 53, 77–86.
- Chng, S.-S., Ruiz, N., Chimalakonda, G., Silhavy, T.J., Kahne, D., 2010. Characterization of the two-protein complex in *Escherichia coli* responsible for lipopolysaccharide assembly at the outer membrane. *Proc. Natl. Acad. Sci. USA* 107, 5363–5368.
- Choi, U., Lee, C.-R., 2019. Distinct roles of outer membrane porins in antibiotic resistance and membrane integrity in *Escherichia coli*. *Front Microbiol* 10, 953.
- Chong, Z.-S., Woo, W.-F., Chng, S.-S., 2015. Osmoporin OmpC forms a complex with MlaA to maintain outer membrane lipid asymmetry in *Escherichia coli*. *Mol. Microbiol.* 98, 1133–1146.
- Chowdhury, F.R., Findlay, B.L., 2023. Fitness costs of antibiotic resistance impede the evolution of resistance to other antibiotics. *ACS Infect. Dis.* 9, 1834–1845.
- Chu, D., Barnes, D.J., 2016. The lag-phase during diauxic growth is a trade-off between fast adaptation and high growth rate. *Sci. Rep.* 6, 25191.
- Cirz, R.T., Chin, J.K., Andes, D.R., Crécy-Lagard, V. de, Craig, W.A., Romesberg, F.E., 2005. Inhibition of Mutation and Combating the Evolution of Antibiotic Resistance. *PLoS Biol.* 3, e176.
- CLSI, 2018. M07: Dilution AST for Aerobically Grown Bacteria. CLSI. (<https://clsi.org/standards/products/microbiology/documents/m07/>). Accessed January 12, 2020.
- Cochrane, S.A., Findlay, B., Vederas, J.C., Ratemi, E.S., 2014a. Key residues in octyl-tridecaptin A1 analogues linked to stable secondary structures in the membrane. *ChemBiochem Eur. J. Chem. Biol.* 15, 1295–1299.
- Cochrane, S.A., Lohans, C.T., Brandelli, J.R., Mulvey, G., Armstrong, G.D., Vederas, J.C., 2014b. Synthesis and structure–activity relationship studies of n-terminal analogues of the antimicrobial peptide Tridecaptin A1. *J. Med. Chem.* 57, 1127–1131.
- Cochrane, S.A., Findlay, B., Bakhtiari, A., Acedo, J.Z., Rodriguez-Lopez, E.M., Mercier, P., Vederas, J.C., 2016. Antimicrobial lipopeptide tridecaptin A1 selectively binds to Gram-negative lipid II. *Proc. Natl. Acad. Sci.* 113, 11561–11566.
- Croze, O.A., Ferguson, G.P., Cates, M.E., Poon, W.C.K., 2011. Migration of chemotactic bacteria in soft agar: role of gel concentration. *Biophys. J.* 101, 525–534.
- Datsenko, K.A., Wanner, B.L., 2000. One-step inactivation of chromosomal genes in *Escherichia coli* K-12 using PCR products. *Proc. Natl. Acad. Sci. USA* 97, 6640–6645.
- Divoux, T., Mao, B., Snabre, P., 2015. Syneresis and delayed detachment in agar plates. *Soft Matter* 11, 3677–3685.
- Einhorn-Stoll, U., 2018. Pectin-water interactions in foods – from powder to gel. *Food Hydrocoll.* 78, 109–119.
- Ge, S.X., Jung, D., Yao, R., 2020. ShinyGO: a graphical gene-set enrichment tool for animals and plants. *Bioinformatics* 36, 2628–2629.
- Ge, Y., MacDonald, D.L., Holroyd, K.J., Thornsberry, C., Wexler, H., Zasloff, M., 1999. In vitro antibacterial properties of pexiganan, an analog of magainin. *Antimicrob. Agents Chemother.* 43, 782–788.
- Ghaddar, N., Hashemidaj, M., Findlay, B.L., 2018. Access to high-impact mutations constrains the evolution of antibiotic resistance in soft agar. *Sci. Rep.* 2018 81, 8, 1–10.
- Grenier, F., Matteau, D., Baby, V., Rodrigue, S., 2014. Complete Genome Sequence of *Escherichia coli* BW25113. *Genome Announc* 2, e01038-14.
- Hart, E.M., Mitchell, A.M., Konovalova, A., Grabowicz, M., Sheng, J., Han, X., et al., 2019. A small-molecule inhibitor of BamA impervious to efflux and the outer membrane permeability barrier. *Proc. Natl. Acad. Sci. USA* 116, 21748–21757.
- Hjort, K., Nicoloff, H., Andersson, D.I., 2016. Unstable tandem gene amplification generates heteroresistance (variation in resistance within a population) to colistin in *Salmonella enterica*. *Mol. Microbiol.* 102, 274–289.
- Huang, L., Wang, M., Mo, T., Liu, M., Biville, F., Zhu, D., et al., 2019. Role of LptD in resistance to glutaraldehyde and pathogenicity in *Riemerella anatipestifer*. *Front Microbiol* 10, 1443.
- Imai, Y., Meyer, K.J., Iinishi, A., Favre-Godal, Q., Green, R., Manuse, S., et al., 2019. A new antibiotic selectively kills gram-negative pathogens. *Nature* 576, 459–464.
- Jacobs, A., 2019. U.N. Issues Urgent Warning on the Growing Peril of Drug-Resistant Infections. *N. Y.* (<https://www.nytimes.com/2019/04/29/health/un-drug-resistance-antibiotics.html>). Accessed August 28, 2022.
- Jouenne, S., 2020. Polymer flooding in high temperature, high salinity conditions: selection of polymer type and polymer chemistry, thermal stability. *J. Pet. Sci. Eng.* 195, 107545.
- Kaur, H., Jakob, R.P., Marzinek, J.K., Green, R., Imai, Y., Bolla, J.R., et al., 2021. The antibiotic darobactin mimics a β -strand to inhibit outer membrane insertase. *Nature* 593, 125–129.
- Laserna, E.C., Uyenco, F., Epifanio, E., Veroy, R.L., Cajipe, G.J.B., 1981. Carrageenan from *Eucheuma striatum* (Schmitz) in media for fungal and yeast cultures. *Appl. Environ. Microbiol.* 42, 174–175.
- Lee, C., Park, C., 2013. Mutations upregulating the flhDC operon of *Escherichia coli* K-12. *J. Microbiol. Seoul. Korea* 51, 140–144.
- Lehman, K.M., Grabowicz, M., 2019. Countering gram-negative antibiotic resistance: recent progress in disrupting the outer membrane with novel therapeutics. *Antibiot. Basel Switz.* 8, 163.
- Li, Y.-X., Zhong, Z., Zhang, W.-P., Qian, P.-Y., 2018b. Discovery of cationic nonribosomal peptides as Gram-negative antibiotics through global genome mining. *Nat. Commun.* 9, 3273.
- Li, Y.-X., Zhong, Z., Hou, P., Zhang, W.-P., Qian, P.-Y., 2018a. Resistance to nonribosomal peptide antibiotics mediated by D-stereospecific peptidases. *Nat. Chem. Biol.* 14, 381–387.
- Liao, W., Lin, J., Jia, H., Zhou, C., Zhang, Y., Lin, Y., et al., 2020. Resistance and Heteroresistance to Colistin in *Escherichia coli* Isolates from Wenzhou, China. *Infect. Drug Resist* 13, 3551–3561.

- Ling, L.L., Schneider, T., Peoples, A.J., Spoering, A.L., Engels, I., Conlon, B.P., et al., 2015. A new antibiotic kills pathogens without detectable resistance. *Nature* 517, 455–459.
- Liu, Y.-F., Yan, J.-J., Lei, H.-Y., Teng, C.-H., Wang, M.-C., Tseng, C.-C., Wu, J.-J., 2012. Loss of outer membrane protein C in *Escherichia coli* contributes to both antibiotic resistance and escaping antibody-dependent bactericidal activity. *Infect. Immun.* 80, 1815–1822.
- Lohans, C.T., Huang, Z., Belkum, M.J. van, Giroud, M., Sit, C.S., Steels, E.M., et al., 2012. Structural characterization of the highly cyclized lantibiotic Paenicidin A via a partial desulfurization/reduction strategy. *J. Am. Chem. Soc.* 134, 19540–19543.
- Luther, A., Urfer, M., Zahn, M., Müller, M., Wang, S.-Y., Mondal, M., et al., 2019. Chimeric peptidomimetic antibiotics against gram-negative bacteria. *Nature* 576, 452–458.
- Manioglou, S., Modaresi, S.M., Ritzmann, N., Thoma, J., Overall, S.A., Harms, A., et al., 2022. Antibiotic polymyxin arranges lipopolysaccharide into crystalline structures to solidify the bacterial membrane. *Nat. Commun.* 13, 6195.
- Martin, J.K., Sheehan, J.P., Bratton, B.P., Moore, G.M., Mateus, A., Li, S.H.-J., et al., 2020. A dual-mechanism antibiotic kills gram-negative bacteria and avoids drug resistance. *Cell* 181, 1518–1532.e14.
- Martinez, J.L., Baquero, F., 2000. Mutation frequencies and antibiotic resistance. *Antimicrob. Agents Chemother.* 44, 1771–1777.
- Mcguire, J.M., Wolfe, R.N., Ziegler, D.W., 1955. Vancomycin, a new antibiotic. II. In vitro antibacterial studies. *Antibiot. Annu* 3, 612–618.
- Murray, C.J., Ikuta, K.S., Sharara, F., Swetschinski, L., Robles Aguilar, G., Gray, A., et al., 2022. Global burden of bacterial antimicrobial resistance in 2019: a systematic analysis. *Lancet* 399, 629–655.
- Pahil, K.S., Gilman, M.S.A., Baidin, V., Clairfeuille, T., Mattei, P., Bieniossek, C., et al., 2024. A new antibiotic traps lipopolysaccharide in its intermembrane transporter. *Nature* 625, 572–577.
- Phan, K., Ferenci, T., 2017. The fitness costs and trade-off shapes associated with the exclusion of nine antibiotics by OmpF porin channels. *ISME J.* 11, 1472–1482.
- Prüss, B.M., Nelms, J.M., Park, C., Wolfe, A.J., 1994. Mutations in NADH:ubiquinone oxidoreductase of *Escherichia coli* affect growth on mixed amino acids. *J. Bacteriol.* 176, 2143–2150.
- Qian, J., Garrett, T.A., Raetz, C.R.H., 2014. In vitro assembly of the outer core of the lipopolysaccharide from *Escherichia coli* K-12 and *Salmonella* Typhimurium. *Biochemistry* 53, 1250–1262.
- Reisch, C.R., Prather, K.L.J., 2015. The no-SCAR (Scarless Cas9 Assisted Recombineering) system for genome editing in *Escherichia coli*. *Sci. Rep.* 5, 15096.
- Reisch, C.R., Prather, K.L.J., 2017. Scarless Cas9 assisted recombineering (no-SCAR) in *Escherichia coli*, an easy-to-use system for genome editing. *Curr. Protoc. Mol. Biol.* 117 (31.8), 1–31, 8.20.
- Reiter, M.A., Vorholt, J.A., 2024. Dashing growth curves: a web application for rapid and interactive analysis of microbial growth curves. *BMC Bioinforma.* 25, 67.
- Salvy, P., Hatzimanikatis, V., 2021. Emergence of diauxie as an optimal growth strategy under resource allocation constraints in cellular metabolism. *Proc. Natl. Acad. Sci.* 118, e2013836118.
- Sánchez, V.E., Bartholomai, G.B., Pilosof, A.M.R., 1995. Rheological properties of food gums as related to their water binding capacity and to soy protein interaction. *LWT - Food Sci. Technol.* 28, 380–385.
- Savinova, T.A., Bocharova, Y.A., Mayansky, N.A., Chebotar, I.V., 2023. Application of dimethicone to prevent culture media from drying in microbiological diagnostics. *Mod. Technol. Med* 15, 14–19.
- Seright, R.S., Henrici, B.J., 1990. Xanthan stability at elevated temperatures. *SPE Reserv Eng.* 5, 52–60.
- Shimada, T., Tanaka, K., 2016. Use of a bacterial luciferase monitoring system to estimate real-time dynamics of intracellular metabolism in *Escherichia coli*. *Appl. Environ. Microbiol.* 82, 5960–5968.
- Shimada, T., Nakazawa, K., Tachikawa, T., Saito, N., Niwa, T., Taguchi, H., Tanaka, K., 2021. Acetate overflow metabolism regulates a major metabolic shift after glucose depletion in *Escherichia coli*. *FEBS Lett.* 595, 2047–2056.
- Shoji, J., Hino, H., Sakazaki, R., Kato, T., Wakisaka, Y., Mayama, M., et al., 1978. Isolation of tridecaptins A, B and C (studies on antibiotics from the genus *Bacillus*. XXIII). *J. Antibiot. (Tokyo)* 31, 646–651.
- Shukla, R., Lavore, F., Maity, S., Derks, M.G.N., Jones, C.R., Vermeulen, B.J.A., et al., 2022. Teixobactin kills bacteria by a two-pronged attack on the cell envelope. *Nature* 608, 390–396.
- Simpson, B.W., Trent, M.S., 2019. Pushing the envelope: LPS modifications and their consequences. *Nat. Rev. Microbiol.* 17, 403–416.
- Sommer, M.O.A., Munck, C., Toft-Kehler, R.V., Andersson, D.I., 2017. Prediction of antibiotic resistance: time for a new preclinical paradigm? *Nat. Rev. Microbiol.* 15, 689–696.
- Srinivas, N., Jetter, P., Ueberbacher, B.J., Werneburg, M., Zerbe, K., Steinmann, J., et al., 2010. Peptidomimetic antibiotics target outer-membrane biogenesis in *Pseudomonas aeruginosa*. *Science* 327, 1010–1013.
- Stokes, J.M., Yang, K., Swanson, K., Jin, W., Cubillos-Ruiz, A., Donghia, N.M., et al., 2020. A deep learning approach to antibiotic discovery. *Cell* 180, 688–702.e13.
- Taylor, P.L., Blakely, K.M., Leon, G.P. de, Walker, J.R., McArthur, F., Evdokimova, E., et al., 2008. Structure and function of sedoheptulose-7-phosphate isomerase, a critical enzyme for lipopolysaccharide biosynthesis and a target for antibiotic adjuvants. *J. Biol. Chem.* 283, 2835–2845.
- Tietgen, M., Semmler, T., Riedel-Christ, S., Kempf, V.A.J., Molinaro, A., Ewers, C., Göttig, S., 2018. Impact of the colistin resistance gene *mcr-1* on bacterial fitness. *Int. J. Antimicrob. Agents* 51, 554–561.
- Trimble, M.J., Mlynářík, P., Kolář, M., Hancock, R.E.W., 2016. Polymyxin: alternative mechanisms of action and resistance. *Cold Spring Harb. Perspect. Med.* 6, a025288.
- Upadhayay, A., Ling, J., Pal, D., Xie, Y., Ping, F.-F., Kumar, A., 2023. Resistance-proof antimicrobial drug discovery to combat global antimicrobial resistance threat. *Drug Resist Updat* 66, 100890.
- Van den Bergh, B., Schramke, H., Michiels, J.E., Kimkes, T.E.P., Radzikowski, J.L., Schimpf, J., et al., 2022. Mutations in respiratory complex I promote antibiotic persistence through alterations in intracellular acidity and protein synthesis. *Nat. Commun.* 13, 546.
- Wang, H., Ishchenko, A., Skudlarek, J., Shen, P., Dzhekueva, L., Painter, R.E., et al., 2024. Cerastecins inhibit membrane lipooligosaccharide transport in drug-resistant *Acinetobacter baumannii*. *Nat. Microbiol.* 9, 1244–1255.
- Wang, X., Wood, T.K., 2011. IS5 inserts upstream of the master motility operon *flhDC* in a quasi-Lamarckian way. *ISME J.* 5, 1517–1525.
- Wang, Y., Luo, Q., Xiao, T., Zhu, Y., Xiao, Y., 2022. Impact of polymyxin resistance on virulence and fitness among clinically important gram-negative bacteria. *Engineering* 13, 178–185.
- Werneburg, M., Zerbe, K., Juhas, M., Bigler, L., Stalder, U., Kaech, A., et al., 2012. Inhibition of lipopolysaccharide transport to the outer membrane in *Pseudomonas aeruginosa* by peptidomimetic antibiotics. *ChemBioChem* 13, 1767–1775.
- WHO publishes list of bacteria for which new antibiotics are urgently needed** (<https://www.who.int/news/item/27-02-2017-who-publishes-list-of-bacteria-for-which-new-antibiotics-are-urgently-needed>). Accessed January 15, 2023.
- Yoshida, M., Reyes, S.G., Tsuda, S., Horinouchi, T., Furusawa, C., Cronin, L., 2017. Time-programmable drug dosing allows the manipulation, suppression and reversal of antibiotic drug resistance *in vitro*. *Nat. Commun.* 8, 15589.
- Zampaloni, C., Mattei, P., Bleicher, K., Winther, L., Thäte, C., Bucher, C., et al., 2024. A novel antibiotic class targeting the lipopolysaccharide transporter. *Nature* 625, 566–571.
- Zhang, X., Li, Y., Wang, W., Zhang, J., Lin, Y., Hong, B., et al., 2019. Identification of an anti-Gram-negative bacteria agent disrupting the interaction between lipopolysaccharide transporters LptA and LptC. *Int. J. Antimicrob. Agents* 53, 442–448.
- Zhao, X., Zhong, X., Yang, S., Deng, K., Liu, L., Song, X., et al., 2023. Elucidating the mechanism of action of the gram-negative-pathogen-selective cyclic antimicrobial lipopeptide brevicidine. *Antimicrob. Agents Chemother.* 67, e00010-23.